Please do not adjust margins

Molecular Systems Design & Engineering

ARTICLE

Capture and immobilisation of Iodine (I_2) utilising polymer-based ZIF-8 nanocomposite membranes

Received 00th January 20xx,
Accepted 00th January 20xx

DOI: 10.1039/x0xx00000x

www.rsc.org/

E. M. Mahdi, Abhijeet K. Chaudhuri, and Jin-Chong Tan*

Abstract

Polymer nanocomposites made up of nanoporous metal-organic frameworks (MOFs) is fast becoming a staple of next generation hybrid composites, and are currently being intensely developed for gaseous capture and separations. This work report the first attempt of the capture and retention of iodine (I_2) using polymer-MOF (ZIF-8) nanocomposites. Membranes of ZIF-8-based nanocomposites (comprising either a glassy Matrimid or a rubbery polyurethane (PU) matrix) were prepared via the colloidal-mixing approach, and its viability for I_2 capture and retention effects were determined through absorption experiments, nanoindentation mechanical measurements, and thermogravimetric (TGA) analysis. The absorption experiments demonstrated that I_2 capture and retention is possible in all of the nanocomposite membranes, although the PU/ZIF-8 30 wt.% nanocomposite exhibited higher affinity for I_2 absorption (>32 wt.%). It is reasoned that the molecular affinity and attraction between I_2, (2-methylimidazolate organic ligands of) ZIF-8 nanoparticle, and the polymer matrices (Matrimid and PU) will catalyse the formation of weak secondary bonds, resulting in the 'capture' and 'retention' of I_2 within molecular segments of the polymers and inside the pores of ZIF-8. The enhancement of the Young's modulus (E) of the PU/ZIF-8 30 wt.% nanocomposite (E increased by ~14 wt.%) is postulated to be due to I_2-rigidification, while TGA analysis proved that I_2 retention within both free volume of the polymer and ZIF-8 sodalite cages remained intact up till the points of structural degradation, at ~200 °C for the PU-based nanocomposites, and at ~300 °C for the Matrimid-based nanocomposites. We propose that the affinity of the organic ligands in ZIF-8 and the formation of free volume in the nanocomposites from the presence of ZIF-8 attracted I_2, and the formation of secondary bonds between these constituents (H-bonds) acted to strengthen not only the nanocomposite, but keeping I_2 from being released despite the larger pore size and gate-opening dynamics of ZIF-8. It was therefore concluded that a combination of nanoparticles of porous MOFs and rubbery polymer are promising for further development to enable I_2 capture and retention applications.

1. Introduction

Nuclear technology is prominent in two sectors that are intrinsic parts of our lives: power generation[1] and medicine.[2] Nuclear power plants (NPP) are regarded as a source of clean, renewable, and cost-effective energy,[3] while nuclear medicine forms the core of many diagnosis techniques and treatments for illnesses plaguing mankind.[4] Nuclear-related processes produce many by-products such as isotopes of iodine (^{129}I and ^{131}I), ^{135}Cs and ^{99}Tc, some of which emit alpha (α), beta (ß), gamma (γ), and neutron (n), all of which are hazardous to humans and the environment. Their extensive half-lives ($t_{1/2}$), some ranging to millions and billions of years, necessitates a permanent and effective disposal approach for these by-products, aptly called nuclear waste products.[5,6]

A common radionuclide that is produced as a by-product of power generation are isotopes of iodine; ^{129}I, with a $t_{1/2}$ of 1.5×10^7 years, which is detrimental to the environment, and ^{131}I, with a $t_{1/2}$ of 8.02 days, which is detrimental to human metabolic processes.[7] As such, many research works has been focused on the successful capture and confinement of iodine.[8,9] Common industrial practice in capturing and storing iodine is dominated by activated carbon[10,11] and zeolites[12] filters and scrubbers; however, recent research work are oriented towards metal-organic frameworks (MOFs)[13,14] or variants of composites,[9,15,16] to varying degrees of success.

MOFs are an emerging class of hybrid materials[17-19] formed by coordinating multifunctional organic linkers to metallic ions or clusters, giving rise to a plethora of 3-D porous networks containing periodic nanosized porosity or extended metal-organic channels.[20-22] The presence of the metallic cores and organic linkers introduce tuneable physico-chemical properties that are absent from purely metallic or purely organic materials;[23] many MOFs are extremely porous (typically >1,000 m^2/g)[24] to accommodate guest encapsulation or host-guest confinement interactions,[25] while certain MOF structures

[a] Department of Engineering Science, Parks Road, University of Oxford, OX1 3PJ, United Kingdom
*Corresponding Author
Electronic Supplementary Information (ESI) available: XRD plots of the blank nanocomposites, raw data pertaining to nanoindentation, and TGA compilation of all the nanocomposites, including ZIF-8 nanoparticles.

Please do not adjust margins

Please do not adjust margins

feature coordinatively unsaturated metal sites[26] that are highly accessible for molecular adsorption. From the mechanical standpoint, the open frameworks of MOFs are relatively more flexible (lower stiffness)[27,28] and also softer compared to their constituents or inorganic structural analogues.[29] A notable example of a MOF that embodies these properties are a subclass called Zeolitic Imidazolate Frameworks (ZIFs),[30] which are structural cousins to inorganic zeolites, an established catalyst in the petrochemical industry. Ag-impregnated zeolites (Ag-MORs)[31] have been used to capture iodine, and filters to that effect are available commercially. ZIFs exhibit a tuneable accessible surface area[30] and a respectably high thermal stability (up to 500 °C),[32] making them ideal candidates for many potential applications.[33-35] Recent reports on the Terahertz lattice dynamics and soft modes of ZIFs[36] may also play a role in guest sorption, retention and delivery.

ZIF-8 [$Zn(mIm)_2$; mIm = 2-methylimidazolate], which is a cubic ZIF material adopting a sodalite architecture (surface area up to 1,950 m^2/g),[32] has been shown to be effective in the capture and retention of iodine in both powdered form or extruded pellets.[7] Despite its reported effectiveness, the deliverability of ZIF-8 remains an open question. Depositing loose powders of ZIF-8 into aqueous environments is clearly not a practical approach for industrial practices.[37] Therefore, recent work has focused on the formation of MOFs, and by extension, ZIF-based composites[38] and membrane systems[39,40] to improve robustness and enhance deliverability. There are plenty of examples of MOFs and ZIFs-based composites,[41,42] encompassing polymer-based and ceramic-based matrices. However, MOF-polymer composites are especially favoured, due to the affinity between the organic ligands of MOFs and the polymer molecules/chains, which results in the formation of strong and continuous structure that retained all of the advantages of MOFs without compromising the structural features associated with polymers. The flexibility and ease of processing of polymers also make them easily deployable and impregnated with MOF nanoparticles at controlled loadings.[43,44] It should also be pointed out that recently reported work suggested that the deployment of composites,[15,16] when exploiting the advantages of both the matrix and fillers, are more effective in capturing and storing iodine compared to either constituents acting on their own.

Previous attempts have been made to capture and immobilise iodine within ZIF-8/HKUST-1, Ag, and glass powders (EG2992 and EG2998), forming a glass-composite material (GCM), which turned out to be a success, as reported by Sava *et al.*[45] Despite the effectiveness of this reported approach, its energy intensiveness and the requirement to employ a mixture of multiple constituents within a single system might prove to be over demanding for practical engineering solutions.

The current study aims to combine the ease of material processability and adaptability of polymers and by leveraging the large surface area and regular pores offered by MOFs to create a composite membrane system, which is structurally resilient, easily deliverable, and mechanically robust to capture and retain iodine. This work aims to develop, assess and characterise the viability of ZIF-8/polymer nanocomposites as an iodine capture and retention model system. Herein, one of the objectives is to also minimise the energy expenditure associated with the capture and retention process, and thus to rely upon the molecular interactions and affinity between iodine, ZIF-8 nanoparticles, and polymer matrices (either glassy or rubbery) to expedite the uptake of iodine into the thin composite membranes. The introduction of this so-called *passive* polymer-based system represents an equally effective alternative that is cost effective and highly deliverable; the concept of which is potentially viable for development to enable industrial applications in the long run.

2. Materials and Methods

2.1 Synthesis of ZIF-8 nanoparticles, and processing of ZIF-8/Matrimid and PU/ZIF-8 nanocomposite membranes

The methods involved in synthesising ZIF-8 nanoparticles (Fig. 1) are reported elsewhere[46] and was replicated in this work. Polyurethane (PU) beads was purchased from Sigma Aldrich, while Matrimid®5218 flakes were supplied by Huntsman Materials (the polymeric structure for the polymers and ZIF-8 are presented in the ESI in Fig. S2). Both polymers were used as is without any further alterations. A measured amount of PU, based on Equation 1, was dissolved in tetrahydofuran (THF), while the same was done for Matrimid flakes in chloroform ($CHCl_3$), so as to achieve a targeted ZIF-8 nanoparticle loading of 30 wt.%.

$$\text{ZIF-8 wt.\%} = \left(\frac{m_{\text{ZIF-8}}}{m_{\text{ZIF-8}} + m_{\text{PU}}} \right) \times 100\% \qquad (1)$$

where $m_{ZIF\text{-}8}$ is the weight (in grams) of ZIF-8 mixed into the colloidal solution, and m_{PU} is the weight (in grams) of the PU beads mixed into the composite solution. m_{PU} can be replaced with m_{Matrimid} in the case of Matrimid flakes.

Both were magnetically stirred for 24 hours, forming a clear and transparent viscous solution for the PU, and a clear yellowish viscous solution for Matrimid. Two vials of ZIF-8 nanoparticles were prepared (~2 g each), dispersed in $CHCl_3$ and THF, and were added to the Matrimid and PU solutions at a measured rate, respectively. The combined PU/ZIF-8 and ZIF-8/Matrimid solution were again magnetically stirred for 24 hours, forming opaque and viscous solutions. The PU/ZIF-8 solution was casted onto a PTFE substrate, while the ZIF-8/Matrimid solution was casted onto a glass substrate using an automated doctor blade machine at a constant speed of 15 mm^{-1}, with the thickness of the doctor blade set to 150 µm. After casting, the membranes were left to slow cure in a glove bag saturated with THF vapour (PU/ZIF-8) and $CHCl_3$ vapour (ZIF-8/Matrimid) for 6 hours; after which they were removed and placed in a vacuum oven and dried for 24 hours at 85 °C to remove any residual THF/$CHCl_3$ within the PU, Matrimid, or ZIF-8 nanoparticles. After drying, the membranes were removed from the vacuum oven and carefully dislodged from the substrate, had its thicknesses measured, and stored for further tests. The methodology described above resembles

 This journal is © The Royal Society of Chemistry 2016

Please do not adjust margins

Please do not adjust margins

that of our recent report to fabricate thin mixed-matrix membranes of MOF/polymer nanocomposites.[44]

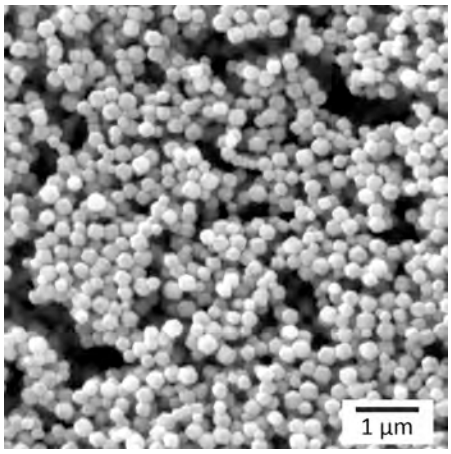

Fig. 1 Scanning electron micrograph showing ZIF-8 nanoparticles prior to being embedded in polymer-MOF nanocomposite. The mean diameter of nanoparticle is *ca.* 150 nm.

2.2 Iodine (I_2) Capture

A solution of 10 mM of iodine (henceforth called I_2) was prepared with cyclohexane (C_6H_{12}) as its base; both were purchased from Sigma Aldrich and used as is without further modifications or purification. The previously synthesised PU/ZIF-8 and ZIF-8/Matrimid nanocomposite were dried in a vacuum oven for 24 hours at 85 °C prior to the I_2 uptake experiments to remove any moisture or solvents remaining on the surface of or within the membranes. These nanocomposites were then carefully weighed, with the weight recorded for every sample. The nanocomposites were then placed in a 50 mL glass vial, and 1 mL of the aforementioned I_2 solution were sampled and placed into the vials and hermetically sealed. The vials were placed away from direct exposure to sunlight in order to prevent UV degradation or from influencing I_2 capture. Images of the vials were taken at designated intervals of 0, 1, 2, 4, 6, 24, 48, 72 and 96 hours. At the end of the uptake experiments, the membranes were removed from the solution, washed, and weighed.

The samples exhibiting the highest level of capture and retention of iodine was used for desorption experiments, where the sample was submerged in ethanol (EtOH) and allowed to desorb for a set amount of time. Images were taken of the desorption experiments to monitor the level of iodine released from the samples. The I_2-absorbing polymers and nanocomposites were subjected to multiple characterisation techniques to confirm its absorptive and retentive capabilities.

2.3 Scanning Electron Microscopy (SEM)

Matrimid, PU, and their corresponding ZIF-8 nanocomposites, as is, were submerged in liquid nitrogen (LN_2) and then fractured at the cross sections to produce a clear view of their through-thickness internal morphology. The fractured samples were mounted on an SEM stub and secured using carbon tapes at a 90° angle. The samples were then sputter-coated with gold for 30 seconds, and were then loaded into the field emission gun SEM (TESCAN LYRA3 FEG-SEM/FIB apparatus) for imaging. Imaging was conducted under a high vacuum (HV mode), at 5-10 kV and employing a magnification of 10,000-30,000×.

2.4 Thermogravimetric Analysis (TGA)

The influence of I_2 uptake towards the thermal and structural modifications of the pristine nanocomposite membranes was studied using the TGA method. The device used in this work is the TGA-Q50 (TA instruments), which comes with its own induction-heating chamber and platinum sample holder. A portion of the nanocomposites were carefully sectioned from the main sample (~1.5 mg), and placed onto the platinum (Pt) sample holder. Prior to the experiments, the sample holder was calibrated to zero weight in order to prevent any foreign particles or objects from influencing the readings. The samples were then subjected to the heat treatment outlined and programmed into the software: heating rate of 10 °C min^{-1}, initial temperature of 50 °C and final temperature of 800 °C. These parameters and temperatures were selected in order to guarantee that the samples (which includes Matrimid, PU, and ZIF-8) undergo the total range of thermal phase change and decomposition. The weight percent (wt.%) variation of the samples were recorded at every temperature interval, and these data were then used to construct thermal decomposition plots of the polymer matrices and their corresponding nanocomposites, with and without I_2 guest molecules.

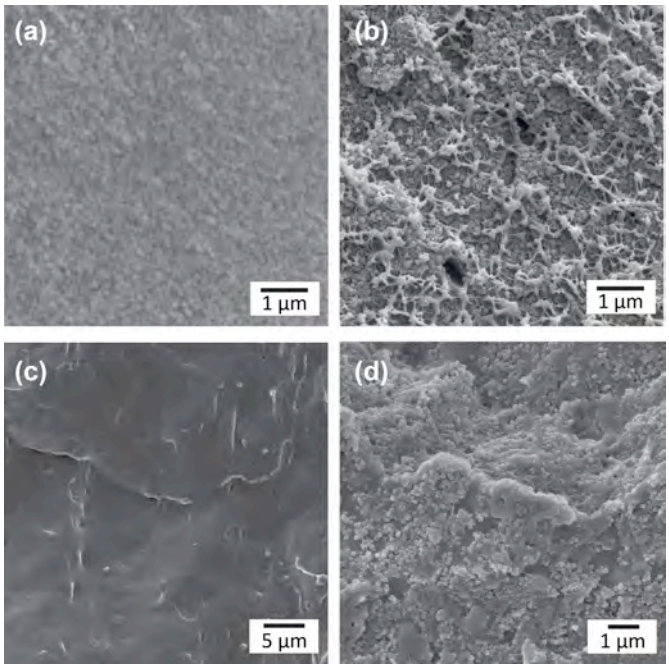

Fig. 2 Cross-sectional SEM images of the polymer and polymer-MOF nanocomposites, with (a) Matrimid, (b) ZIF-8/Matrimid 30 wt.%, (c) PU, and (d) PU/ZIF-8 30 wt.%.

Please do not adjust margins

Please do not adjust margins

2.5 Nanoindentation Mechanical Characterisation

The blank and I_2-loaded nanocomposites were secured onto an aluminium stub using a mounting wax, and their quasi-static nanomechanical properties, specifically the corresponding Young's modulus (*E*) and nanohardness (*H*), were determined using the nanoindentation method *via* the MTS NanoIndenter XP (Agilent Technologies, USA), equipped with a Berkovich three-sided pyramid diamond tip. A collection of 20 indents (at a depth of 2,000 nm) were made per sample at random locations on the membrane surface, as per the method described in Mahdi *et al.*[44]

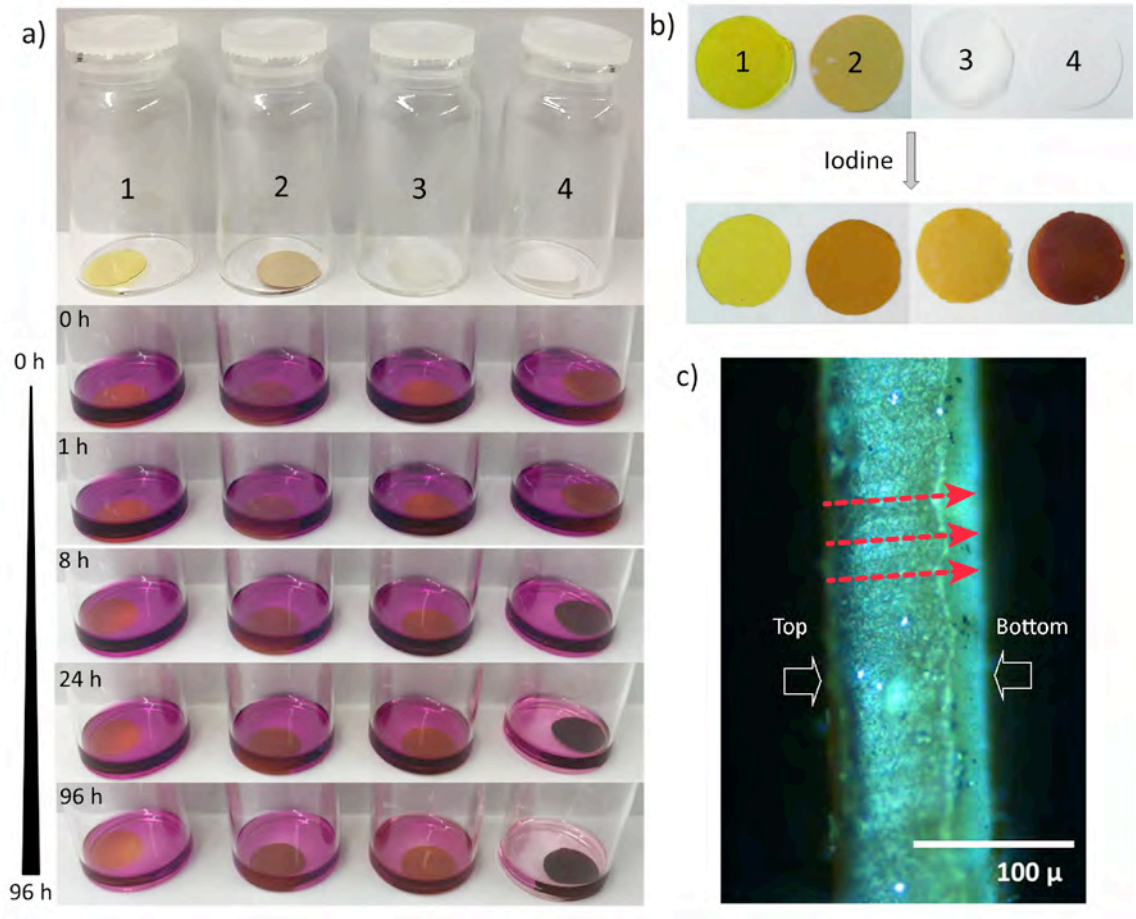

Fig. 3 Determination of I_2 absorption characteristics in the polymer-MOF nanocomposites. (a) The time it took for the composites to absorb I_2 up to 96 hours exposure, where (1) Matrimid, (2) Matrimid/ZIF-8 30 wt.%, (3) PU, and (4) PU/ZIF-8 30 wt.%. (b) Membranes before absorption of I_2 (top) and after absorption of I_2 (bottom). (c) Optical micrographs taken at the cross section of the PU/ZIF-8 30 wt.% membranes, where the dotted arrows indicate the I_2 flow gradient entering the composites. The darker region corresponds to the top membrane surface while the lighter region is the bottom surface (with respect to (a)). It can be seen that the mean membrane thickness is 100 µm.

3. Results and Discussion

3.1 Iodine uptake, immobilisation and release rates

Fig. 2 shows the cross-sectional images of the membranes. It is clear from the SEM images that the dispersion of the ZIF-8 nanoparticles throughout the polymer matrices is uniform. It should also be pointed out that the ZIF-8 nanoparticles embedded in Matrimid are *encapsulated* by Matrimid, exhibiting spherically coated surfaces,[44] while the ZIF-8 nanoparticles *embedded* onto PU seems to retain its original rhombic dodecahedron crystal configuration,[47] further increasing accessibility to the ZIF-8 within the nanocomposite, which is important *vis-à-vis* I_2 capture and retention. The presence of ZIF-8 was also confirmed *via* X-ray diffraction performed on the membranes (see XRD in ESI, Fig. S1).

Fig. 3 shows the vials containing the Matrimid and PU-based ZIF-8 membranes, filled with I_2, at designated time intervals (0-96 hr), while Fig. 4 shows the quantitative uptake capacity of the membranes, as measured by the wt.% of absorbed I_2.

The physical changes to the PU and PU-based nanocomposite is rather pronounced, with PU exhibiting a yellowish tinge, while the PU/ZIF-8 30 wt.% membrane show a deep purple tinge (Fig. 3b). The colour changes are attributed to the absorbed I_2. Data in Fig. 4 shows that the PU/ZIF-8 30 wt.% nanocomposites show a substantial weight gain of 32.4 wt.%, while PU show a much smaller increase of 5.9 wt.%. It

 This journal is © The Royal Society of Chemistry 2016

Please do not adjust margins

Please do not adjust margins

can be seen that higher concentrations of absorbed I_2 will result in the nanocomposites exhibiting a similar colour to that of I_2, while lower absorbed concentrations will result in a light brownish tinge. Due to the relatively small amount of absorbed I_2 in the Matrimid-based membranes (1.8 wt.% and 2.7 wt.% for Matrimid and Matrimid/ZIF-8 30 wt.%, respectively), their corresponding colours post-absorption remained similar (Fig. 3b). It was evident that the uptake and retention of I_2 resulted in change to the colours of the polymers and their corresponding nanocomposites.

To confirm I_2 capture *within* the nanocomposite as opposed to mere surface coverage of I_2, we visually assessed the cross-section of the I_2-loaded composite (Fig. 3c). Optical images taken of the cross-section of the nanocomposite capturing the highest amount of I_2, i.e. PU/ZIF-8 30 wt.%, exhibited features suggestive of I_2-transport across the nanocomposite interior. Colour gradient in Fig. 3c indicates the direction of the flow of I_2, proving that I_2 was indeed absorbed by the nanocomposite as opposed to only being present on the surface layer of the composites. Notably the top and bottom surfaces of the nanocomposites could be easily distinguished. It can be seen that the top surface that was exposed to I_2 exhibited a darker shade of purple, as opposed to the bottom surface of the membrane sample. This differential colouration phenomenon elucidates that a concentration gradient is present in the composite, thus indicating that I_2 has infiltrated the nanocomposite but remained entrapped within as opposed to being filtered out of the membrane.

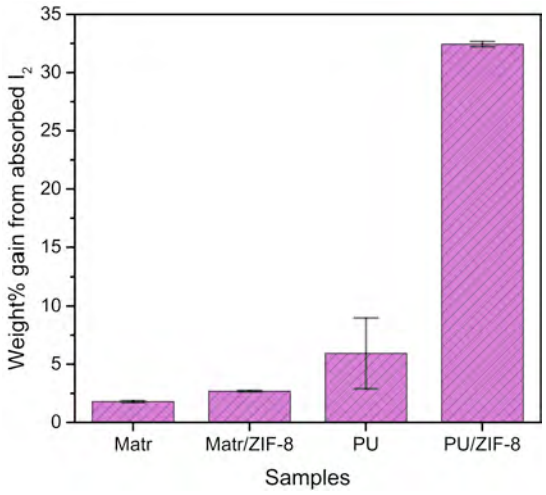

Fig. 4 Weight differential of I_2-uptake in the polymer and 30 wt.% nanocomposite samples. It was found that the weight uptake of I_2 in the Matrimid and its composite is relatively small compared to that of PU and its corresponding nanocomposites.

We examined the I_2 release characteristics by monitoring the change in colour of the solution, where I_2-loaded PU/ZIF-8 30 wt.% nanocomposite was immersed and hermetically sealed. The polymer matrices, as discussed previously, decrease the accessibility to the high surface area of ZIF-8 nanoparticles, which extended the I_2 release time (beyond 6.5 hr), relative to the case of (loose) MOF powders, where a substantial release of captured I_2 was reported after only two hours.[48] Furthermore, the hydrophobicity of the polymer matrices prevented access of polar solvents to the nanoporosity of the ZIF-8 nanoparticles, allowing the nanocomposites to retain I_2 within its microstructure. This was proven by immersing the I_2-loaded PU/ZIF-8 30 wt.% into water, and after a period of 10 days (see Fig. S3 in ESI), there were no colour changes detected in the surrounding water, signifying that I_2 remained immobilised. Importantly, this result shows that despite the affinity of I_2 towards polar solvents (e.g. water), in fact the desorption of I_2 can be suppressed by encapsulating them within a polymer/MOF nanocomposite where the matrix is an intrinsically hydrophobic phase. We reasoned that the complex microstructure of the nanocomposite (Fig. 2) further prevented open access to the adsorption sites located inside the sodalite cages of ZIF-8,[7] such that the absorbed I_2 can remain immobilised within the membrane.

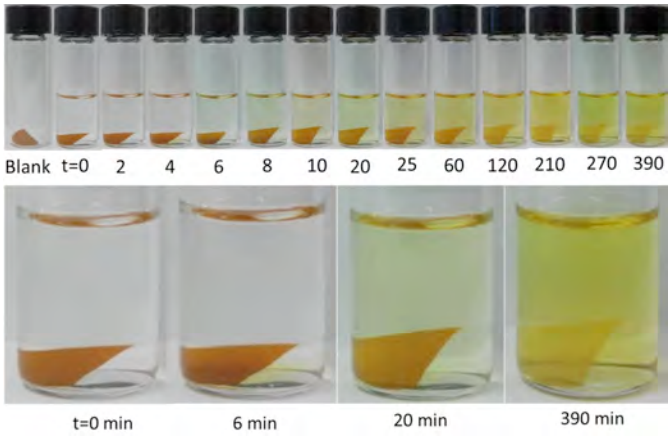

Fig. 5 Iodine release was investigated by monitoring the change in the colour of ethanolic solution in I_2-loaded PU/ZIF-8 30 wt.% at different time points. Since the polymer matrix in nanocomposite decreased accessibility to the high surface area of ZIF-8 pores, I_2 release in ethanol was observed to slow down and remained virtually unchanged beyond 6.5 hr (see ESI Fig.S3 for sample after 10 days of immersion time).

3.2 Nanoindentation properties

The nanoindentation technique was used to characterise the nanomechanical properties of the polymers and their corresponding nanocomposites pre- and post-I_2 absorption. The results are summarised in Fig. 6.

The application of the nanoindentation technique is a practical choice: bulk-testing approaches such as uniaxial tensile test of the membranes will result in the bulk properties (in this case; the matrix of the nanocomposites) being determined. The influence of the nanoparticles (ZIF-8) will subsequently be overlooked. The nanoindentation technique makes measured indents onto minute areas of the surface of the samples at controlled depths (up to ~2 μm),[44,49] enabling it to interrogate the delicate surface regions where the ZIF-8 nanoparticles, the polymer matrices, and incidentally, the absorbed I_2, are actually interacting. For the polymer matrices, this translates into probing the surface where the polymeric chains and I_2 are interacting. This method will allow us to measure relatively small mechanical property differences, more precisely capturing the change in Young's modulus (elastic stiffness) and hardness (resistance against plastic

Please do not adjust margins

Please do not adjust margins

deformation) of the ZIF-8 mixed-matrix membranes due to its absorption of I_2.

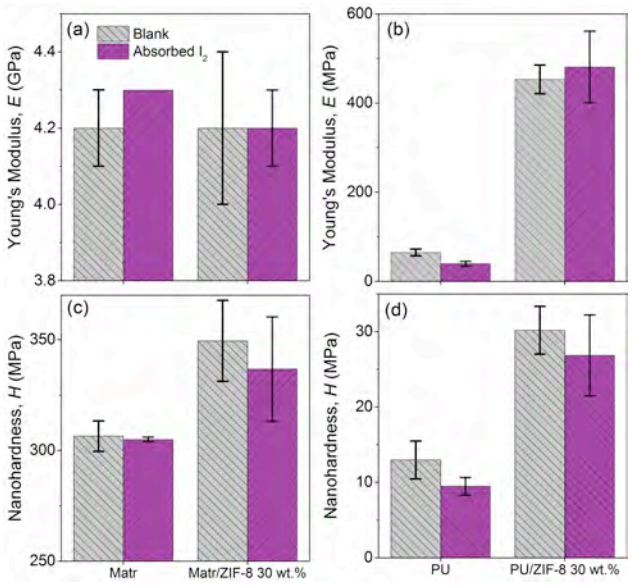

Fig. 6 Nanoindentation results of the Matrimid and PU-based nanocomposite membranes. (a & b) Young's modulus of Matrimid-based and PU-based membranes, respectively. (c & d) Nanohardness of Matrimid-based and PU-based membranes, respectively. Note that glassy Matrimid matrix (whose T_g > room temperature, RT) is significantly stiffer and harder than the rubbery matrix of PU (T_g < RT). Specifically for the blank samples, we note the fall in the Young's modulus of Matrimid/ZIF-8 30 wt.% compared with pristine Matrimid is associated with the incorporation of the ZIF-8 fillers (E_{ZIF-8} ~3 GPa),[28] which are more compliant than the Matrimid phase; this effect has been explained in detail in recent reports.[44,50] The nanoindentation data shown here were averaged from a surface penetration depth ranging from 1 to 2 μm.

Fig. 6 (a) and (c) show that the nanomechanical properties of the Matrimid-based membranes are only slightly affected by the absorption of I_2. This is reflected by the fact that the Young's Modulus (*E*) differs by ~2% for Matrimid and no change was detected for its nanocomposite samples. While for the hardness (*H*) values, the error bars for both samples are within range of each other, implying that the amount of I_2 absorbed by the Matrimid-based membranes are relatively small (all changes falls under the ~5% range) vis-à-vis the nanomechanical properties. The *glassy* nature of the Matrimid matrix at room temperature (Matrimid glass transition temperature, T_g ~345 °C)[51] is important and may account for this outcome. It is envisaged that the molecular packing and rigidity underpinning the polymeric chains of Matrimid form an interconnected network that is sufficiently dense, thereby preventing the infiltration and uptake of I_2 guest molecules. We found that introduction of ZIF-8 nanoparticles (fillers) into Matrimid, despite its expected disruption to the molecular packing of Matrimid,[30,31] in fact did little to boost the overall I_2 absorptive capabilities; thus its marginal impact on the nanomechanical properties of Matrimid-based membranes.

However, a different trend was observed in the PU-based membranes (Figs. 6b & 6d). It is seen that the Young's modulus (*E*) and nanohardness (*H*) values changed by a discernible amount for neat PU (-25.5 MPa, corresponding to ~40% drop for *E*, and -3.5 MPa for *H*, corresponding to a drop of ~27%); and PU/ZIF-8 30 wt.% (28 MPa for *E*, corresponding to an increase of ~6%, and 3 MPa for *H*, corresponding to a decrease of ~11%) post-I_2 absorption. It should be pointed out that unlike in neat Matrimid, the nanomechanical properties in the neat PU sample displayed a contradictory behaviour where *E* and *H* values declined with absorption of I_2. This softening effect is speculated to be due to pervasiveness of I_2 into the hard and soft segments of PU (see ESI Fig.S2), which increased the interatomic distance between the polymeric chain, thus weakening the inter- and intra-molecular bonding interactions affecting its structural integrity.[34] We also propose that the looser molecular packing of the *rubbery* PU polymeric chain (T_g < RT) and nominal molecular attachment of the ZIF-8 to the PU matrix accounted for increased absorption of I_2 into the PU/ZIF-8 30 wt.% nanocomposite, due to increased accessibility to ZIF-8 nanoparticles. The infiltration and I_2 uptake within the ZIF-8 nanoparticles will be assisted by the size of the porous cages of ZIF-8[52] (11.4 Å against the size of iodine molecule of 5.6 Å), if the (loosely packed) rubbery polymer chains may provide an open pathway to reach the ZIF-8 pores, thereby boosting total I_2 uptake (see Fig. 4). Our results show that, for the PU/ZIF-8 30 wt.% nanocomposites upon I_2 absorption there is no major variation detected in *E* and *H*, both of which appear to lie within the respective statistical errors.

3.3 Thermogravimetric analyses (TGA) of the I_2-absorbed nanocomposite membranes

Fig. 7 shows the TGA profiles of the absorbed nanocomposite membranes and their blank counterparts. It is seen from Fig. 7 (a)-(b) that the absorption by the Matrimid-based nanocomposites is almost negligible, as the profile of the absorbed sample is almost identical to the blank sample, with almost minute variations throughout the thermal decomposition profile. This is supported by the weight uptake differential data in Fig. 4, where the wt.% changes post-I_2 absorption for the Matrimid-based nanocomposites remained under 3%.

On the contrary, as per Fig. 4, there is a marked rise in weight change (+32.4%) in the PU/ZIF-8 30 wt.% composite, which is also reflected in the thermal decomposition profile of PU and PU-based nanocomposites. For PU, at ~210 °C, the I_2-loaded composite began decomposing. This is speculated to be due to the initiation of thermal degradation of organics, and with PU molecular structure degradation, the I_2-bonded to the soft segment of the PU polymeric chain is being released. It should also be pointed out that the flash point of I_2 is at 184.3 °C; however, I_2 only began evaporating from PU at 210 °C, meaning that host-guest interactions from being entrapped in PU are shielding I_2 from evaporating at its characteristically lower temperature stated above. We proposed that only when the chain integrity of PU was compromised that, I_2 was exposed to surrounding thermal conditions thus triggering its evaporation process.

 This journal is © The Royal Society of Chemistry 2016

Please do not adjust margins

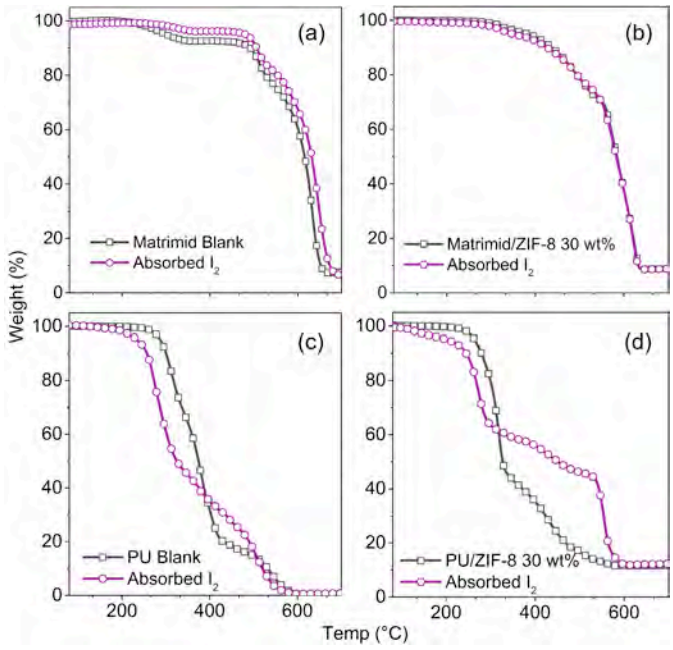

Fig. 7 TGA plots of the (a) Matrimid, (b) ZIF-8/Matrimid 30 wt.%, (c) PU, and (d) PU/ZIF-8 30 wt.%, with their respective blank counterparts. For an overall combined plots of TGA, including the ZIF-8 nanoparticles, refer to Fig. S5 in the ESI.

The thermal decomposition of the I_2-loaded sample was more rapid compared to its blank counterpart. The decomposition of the hard segment of the PU appeared to begin at 310 °C for the I_2-loaded sample, which is earlier than the blank sample, where it began decomposing at 405 °C. The reason for this is that the I_2 loaded sample has formed an intrinsic part of the microstructure of the PU, and once I_2 began to be liberated from the hard segments (ESI Fig. S2) due to structural degradation from the soft segments, the structural integrity of the hard segment begin degrading also, in conjunction with released I_2. A similar trend was observed in the PU/ZIF-8 30 wt.% nanocomposite, where thermal decomposition of the loaded composite began a lot sooner than the blank nanocomposite, however, it is unique in that I_2 is released from the decomposed soft segment of PU and decomposing ZIF-8 (~350 °C, see ESI Fig. S5). Results in Fig. 3 suggest that I_2 is absorbed into ZIF-8 cages as well as the soft and hard segments of PU. Upon thermal decomposition of the PU, ZIF-8 nanoparticles are exposed, and the organic ligands forming bonds with I_2 and the hard segment of PU will began decomposing, releasing I_2 and breaking the chemical and physical interactions formed with PU.

The phenomenon surrounding the release of I_2 from ZIF-8 cages is obvious in Fig. 7d, where from 300-550 °C, the I_2-loaded samples were decomposing at a rate that is slower than its blank counterpart. This can be attributed to the entrapped I_2 in the ZIF-8 cages being released as the ZIF-8 cages are collapsing because of thermal decomposition.[53] At 550 °C, when I_2 was completely removed, a sharp drop was observed in the wt.% of the nanocomposite. Subsequently at 600 °C, its thermal decomposition profile matched that of its blank counterpart, showing that all the entrapped I_2 was indeed removed from both PU and ZIF-8. What is important to establish here is that, by comparing Fig. 7c to 7d, there is strong evidence supporting the notion that thermal stability of the I_2-absorbed PU/ZIF-8 nanocomposite has significantly improved as a consequence of guest immobilisation (§3.4).

3.4 Proposed mechanism responsible for iodine absorption and immobilisation in MOF-polymer nanocomposite membranes

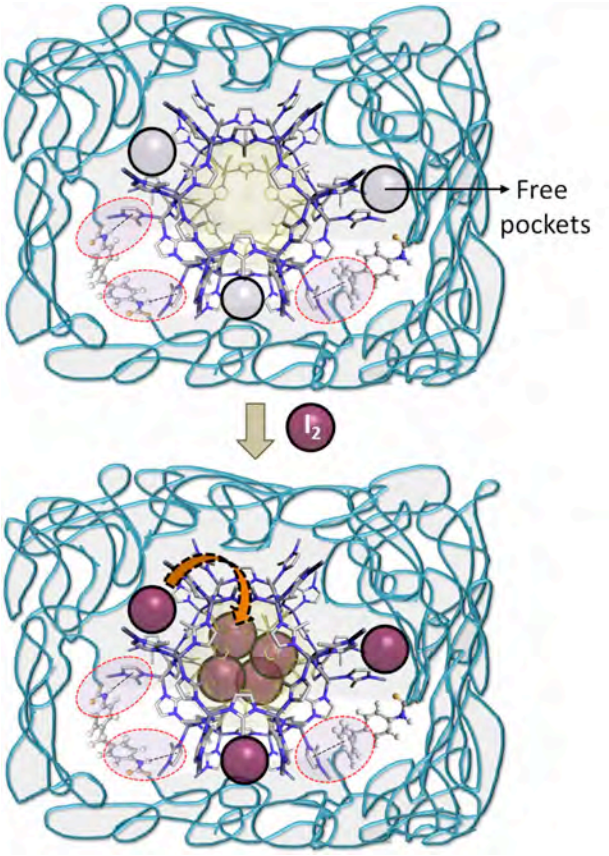

Fig. 8 The proposed I_2 absorption mechanism by the polymer-MOF nanocomposite. The introduction of ZIF-8 nanoparticle within the polymer matrix offer porosity attributed to intrinsic sodalite cages of ZIF-8 (filler phase) and free volumes arising from disruption of the molecular packing of the nanocomposite by the nanoparticle fillers. These voids could serve as active sites, attracting I_2 molecules and forming bonds with the mIm ligands of ZIF-8, and the 'hard' and 'soft' segments of the PU (see ESI Fig.S2) or the active coordination sites present in Matrimid.[44]

Fig. 8 illustrates the proposed absorption mechanism that explains I_2 uptake and retention by the polymer-MOF nanocomposites. Based on the observed I_2 uptake by the polymers and their corresponding ZIF-8 nanocomposites, we propose that the uptake of iodine will be made more efficient with the utilisation of a flexible polymeric molecular backbone. The high surface area of ZIF-8 nanoparticles (~1,650 m^2 g^{-1})[54] are expected to offer significant active sites to afford adsorption of I_2,[55] mostly *via* combined actions of chemisorption[56] and physisorption;[7] however, retention of the adsorbate is significantly strengthened by the polymer matrices. Both polymers (Matrimid and PU) exhibited almost negligible amounts of I_2 uptake (Fig. 4), and it is presumed that

Please do not adjust margins

the high uptake shown by the composites (especially PU/ZIF-8 30 wt.%) is due to I_2 entering the pores of ZIF-8 nanoparticles instead of the free volume within the polymers formed by the presence of the nanoparticles. However, the presence of functional groups and aromatic moieties in both Matrimid and PU are potential sites for the weak molecular interactions with I_2 molecules, therefore, the possibility of I_2 storage within inter-polymer-MOF pockets (free volume) cannot be completely ruled out. The presence of these unoccupied pockets could also potentially serve as active molecular flexible pathways that allow for the I_2 to infiltrate the composites and guide the molecules towards the more active and high-surface area ZIF-8 nanoparticles cages.

Figure 8 details the plausible molecular level interactions between I_2, ZIF-8, and the polymers (PU in the diagram) in the ZIF-8 nanocomposite. The light yellow spheres indicate the voids formed by the presence of ZIF-8 nanoparticles, while the black circles represents the inter-polymer-ZIF-8 pockets. These free volumes could be of large and small dimensions, which is incidentally not necessary for strong interactions with I_2 when compared to the continuous array of ordered active voids of the ZIF-8 nanoparticles. Smaller volume voids with higher surface area may result in stronger nanoscale confinement with incoming foreign guest species, such as I_2. This effect could be investigated in greater detail by means of, for example positron annihilation lifetime spectroscopy (PALS).[54,57]

Furthermore, comparing the chemical structures of the polymer matrices could provide additional insights into their potential role in the capture and retention of I_2 within ZIF-8 polymer nanocomposites. PU is made up of amide linkages that are suitable for non-covalent interactions, while its flexible ether moiety could potentially provide sites for strong interaction and catalyse molecular dynamics within the matrix that improves small guest molecular mobility. However, in the case of Matrimid, its rigid aromatic backbone could potentially hinder the formation of inter-polymer-ZIF-8 pockets *via* its strong interchain aromatic interactions.

It is clear from our experimental data that the PU samples are more susceptible to I_2 uptake compared to the Matrimid samples. We reasoned that the intrinsic porosity of PU and its ability to interact with guest species *via* weak interactions could explain these differences. Molecular flexibility of the PU's primary chain allows for entropic dynamics of its rubbery structure to capture I_2 more rapidly. On the contrary, tightly packed structural configurations, which is especially prevalent in Matrimid (glassy phase) could result in a lower accessible surface area, rendering them less effective for I_2 immobilisation. The introduction of ZIF-8 nanoparticles into both polymer matrices will create strong "anchoring sites" and increase the free volume (due to disruption to molecular packing) that will enhance the resulting nanocomposites capacity to immobilise I_2. On this basis, the model we proposed in Figure 8 represents the most probable capture and storage mechanism for the Matrimid/ZIF-8 30 wt.% and the PU/ZIF-8 30 wt.% nanocomposites developed in this work.

4. Conclusions

This work represents the first reported attempt of capturing and retaining iodine within membranes made from ZIF-8/polymer nanocomposites. A few conclusions can be drawn from the body of this work, as listed below.

- Iodine was indeed captured and retained within the pristine polymer membranes (albeit at small wt.%), but the immobilisation of I_2 in nanocomposite is prominent particularly in the case of PU/ZIF-8 30 wt.% membranes.
- We identified the rubbery polymer matrix (e.g. PU) results in better absorptive and retention capabilities, which could be associated with the more accessible ZIF-8 pores to afford physisorption and chemisorption processes and further accompanied by physical confinement inside free volumes of the polymers.
- We projected that the mechanism that allowed iodine to be captured and retained within the polymers and nanocomposites can be attributed to the molecular interactions and affinity between the mIm (deprotonated ligand of HmIm) of ZIF-8, iodine molecules, and parts of the polymeric chains of the matrices. Therefore, this passive process requires almost no injection of external energy, but relying completely on molecular and chemical affinities existing between the multiple organic-inorganic molecular constituents in the nanocomposite.
- The formation of ZIF-8/polymer nanocomposites improved the deliverability of the samples and allowed the retention of I_2 at temperatures far beyond its flashpoint, thus boosting thermal stability as evidenced from the TGA experiments.
- Initial design proposal in the context of iodine capture and retention would suggest that a combination between highly porous MOFs containing strong sorption sites (e.g. ZIFs,[30] MILs,[58,59] CuBTC,[60] CPOs[61,62] etc) and rubbery polymers, such as PU, polydimethylsiloxane (PDMS) and polyisobutylene (PIB) will be favourable for maximising iodine capture rates in emerging class of MOF-based mixed-matrix membrane (MMM)[39,63,64] nanocomposites.
- There is a huge scope for future developments in the aforementioned areas, not only to better elucidate the underpinning physico-chemical mechanisms but also to design and tune suitable combinations membrane nanocomposites to yield bespoke guest immobilisation capacities.

Acknowledgements

E.M. Mahdi would like to thank Yayasan Khazanah (YK) for DPhil scholarship that fund his research work at Oxford University. We acknowledge the Royal Society Research Grants (RG140296) for equipment funding. The authors thank Mr. S. Ying and Prof. A.M. Korsunsky for access to the Scanning Electron Microscope facilities (MBLEM Laboratory at Oxford, EU FP7 Project iSTRESS (604646)), and to Prof. Steve Roberts and Dr. David Armstrong for usage of nanoindentation facilities at Oxford Materials. We acknowledge the provision of advanced materials characterisation facilities, including TGA, by

 This journal is © The Royal Society of Chemistry 2016

Please do not adjust margins

Please do not adjust margins

the Research Complex at Harwell (RCaH), Rutherford Appleton Laboratory (RAL), Oxfordshire. We thank Dr. Marek Jura and Dr. Gavin Stenning at R53 Materials Characterisation Laboratory in ISIS RAL, for access to the Rigaku X-ray diffractometer.

References

1. A. Verbruggen, E. Laes and S. Lemmens, *Renew. Sust. Energy Rev.*, 2014, **32**, 16-28.
2. V. S. Ramos, V. R. Crispim and L. E. Brandao, *Appl. Radiat. Isot.*, 2013, **82**, 111-118.
3. V. H. M. Visschers, C. Keller and M. Siegrist, *Energy Policy*, 2011, **39**, 3621-3629.
4. L. G. Carneiro, E. A. de Lucena, C. d. S. Sampaio, A. L. Dantas, W. O. Sousa, M. S. Santos and B. M. Dantas, *Appl. Radiat. Isot.*, 2015, **100**, 70-74.
5. R. P. Rechard, J. H. Lee, E. L. Hardin and C. R. Bryan, *Reliab. Eng. Syst. Safe.*, 2014, **122**, 145-164.
6. A. Salama, M. F. El Amin and S. Sun, *Prog. Nucl. Energ.*, 2015, **85**, 747-755.
7. D. F. Sava, M. A. Rodriguez, K. W. Chapman, P. J. Chupas, J. A. Greathouse, P. S. Crozier and T. M. Nenoff, *J. Am. Chem. Soc.*, 2011, **133**, 12398-12401.
8. D. F. Sava, K. W. Chapman, M. A. Rodriguez, J. A. Greathouse, P. S. Crozier, H. Zhao, P. J. Chupas and T. M. Nenoff, *Chem. Mater.*, 2013, **25**, 2591-2596.
9. S. Ma, S. M. Islam, Y. Shim, Q. Gu, P. Wang, H. Li, G. Sun, X. Yang and M. G. Kanatzidis, *Chem. Mater.*, 2014, **26**, 7114-7123.
10. O. B. Yang, J. C. Kim, J. S. Lee and Y. G. Kim, *Ind. Eng. Chem. Res.*, 1993, **32**, 1692-1697.
11. H. Sun, P. La, Z. Zhu, W. Liang, B. Yang and A. Li, *J. Mater. Sci.*, 2015, **50**, 7326-7332.
12. K. W. Chapman, P. J. Chupas and T. M. Nenoff, *J. Am. Chem. Soc.*, 2010, **132**, 8897-8899.
13. B. Assfour, T. Assaad and A. Odeh, *Chem. Phys. Lett.*, 2014, **610-611**, 45-49.
14. C. Falaise, C. Volkringer, J. Facqueur, T. Bousquet, L. Gasnot and T. Loiseau, *Chem. Commun.*, 2013, **49**, 10320-10322.
15. G. Massasso, J. Long, J. Haines, S. Devautour-Vinot, G. Maurin, A. Grandjean, B. Onida, B. Donnadieu, J. Larionova, C. Guerin and Y. Guari, *Inorg. Chem.*, 2014, **53**, 4269-4271.
16. G. Massasso, M. Rodriguez-Castillo, J. Long, A. Grandjean, B. Onida, Y. Guari, C. Guerin and J. Larionova, *J. Mater. Chem. A*, 2015, **3**, 179-188.
17. H. C. Zhou, J. R. Long and O. M. Yaghi, *Chem. Rev.*, 2012, **112**, 673-674.
18. J. C. Tan and B. Civalleri, *CrystEngComm*, 2015, **17**, 197-198.
19. H. Furukawa, K. E. Cordova, M. O'Keeffe and O. M. Yaghi, *Science*, 2013, **341**, 1230444.
20. S. Kitagawa, R. Kitaura and S. Noro, *Angew. Chem. Int. Ed. Engl.*, 2004, **43**, 2334-2375.
21. P. Silva, S. M. Vilela, J. P. Tome and F. A. Almeida Paz, *Chem. Soc. Rev.*, 2015, **44**, 6774-6803.
22. S. Galli, N. Masciocchi, V. Colombo, A. Maspero, G. Palmisano, F. J. Lopez-Garzon, M. Domingo-Garcia, I. Fernandez-Morales, E. Barea and J. A. R. Navarro, *Chem. Mater.*, 2010, **22**, 1664-1672.
23. A. K. Cheetham, C. N. Rao and R. K. Feller, *Chem. Commun.*, 2006, 4780-4795.
24. G. Férey, *Chem. Soc. Rev.*, 2008, **37**, 191-214.
25. M. D. Allendorf, M. E. Foster, F. Leonard, V. Stavila, P. L. Feng, F. P. Doty, K. Leong, E. Y. Ma, S. R. Johnston and A. A. Talin, *J. Phys. Chem. Lett.*, 2015, **6**, 1182-1195.
26. P. D. Dietzel, R. E. Johnsen, R. Blom and H. Fjellvag, *Chem. Eur. J.*, 2008, **14**, 2389-2397.
27. J. C. Tan and A. K. Cheetham, *Chem. Soc. Rev.*, 2011, **40**, 1059-1080.
28. J. C. Tan, B. Civalleri, C. C. Lin, L. Valenzano, R. Galvelis, P. F. Chen, T. D. Bennett, C. Mellot-Draznieks, C. M. Zicovich-Wilson and A. K. Cheetham, *Phys. Rev. Lett.*, 2012, **108**, 095502.
29. J. C. Tan, T. D. Bennett and A. K. Cheetham, *Proc. Natl. Acad. Sci. USA*, 2010, **107**, 9938-9943.
30. A. Phan, C. J. Doonan, F. J. Uribe-Romo, C. B. Knobler, M. O'Keeffe and O. M. Yaghi, *Accounts Chem. Res.*, 2010, **43**, 58-67.
31. T. M. Nenoff, M. A. Rodriguez, N. R. Soelberg and K. W. Chapman, *Microporous Mesoporous Mat.*, 2014, **200**, 297-303.
32. K. S. Park, Z. Ni, A. P. Cote, J. Y. Choi, R. Huang, F. J. Uribe-Romo, H. K. Chae, M. O'Keeffe and O. M. Yaghi, *Proc. Natl. Acad. Sci. USA*, 2006, **103**, 10186-10191.
33. S.-L. Li and Q. Xu, *Energy Environ. Sci.*, 2013, **6**, 1656.
34. S. N. Wijenayake, N. P. Panapitiya, S. H. Versteeg, C. N. Nguyen, S. Goel, K. J. Balkus, I. H. Musselman and J. P. Ferraris, *Ind. Eng. Chem. Res.*, 2013, **52**, 6991-7001.
35. M. R. Ryder and J. C. Tan, *Mater. Sci. Tech.*, 2014, **30**, 1598-1612.
36. M. R. Ryder, B. Civalleri, T. D. Bennett, S. Henke, S. Rudić, G. Cinque, F. Fernandez-Alonso and J. C. Tan, *Phys. Rev. Lett.*, 2014, **113**, 215502.
37. J. Caro, *Curr. Opin. Chem. Eng.*, 2011, **1**, 77-83.
38. N. Stock and S. Biswas, *Chem. Rev.*, 2012, **112**, 933-969.
39. B. Zornoza, C. Tellez, J. Coronas, J. Gascon and F. Kapteijn, *Microporous Mesoporous Mat.*, 2013, **166**, 67-78.
40. L. Diestel, N. Wang, B. Schwiedland, F. Steinbach, U. Giese and J. Caro, *J. Membr. Sci.*, 2015, **492**, 181-186.
41. H. B. Tanh Jeazet, C. Staudt and C. Janiak, *Dalton Trans.*, 2012, **41**, 14003-14027.
42. T. Yang, G. M. Shi and T.-S. Chung, *Adv. Energy Mater.*, 2012, **2**, 1358-1367.
43. Q. Song, S. K. Nataraj, M. V. Roussenova, J. C. Tan, D. J. Hughes, W. Li, P. Bourgoin, M. A. Alam, A. K. Cheetham, S. A. Al-Muhtaseb and E. Sivaniah, *Energy Environ. Sci.*, 2012, **5**, 8359.
44. E. M. Mahdi and J. C. Tan, *J. Membr. Sci.*, 2016, **498**, 276-290.
45. D. F. Sava, T. J. Garino and T. M. Nenoff, *Ind. Eng. Chem. Res.*, 2012, **51**, 614-620.
46. J. Cravillon, S. Münzer, S.-J. Lohmeier, A. Feldhoff, K. Huber and M. Wiebcke, *Chem. Mater.*, 2009, **21**, 1410-1412.
47. Y. C. Pan, D. Heryadi, F. Zhou, L. Zhao, G. Lestari, H. B. Su and Z. P. Lai, *CrystEngComm*, 2011, **13**, 6937-6940.
48. S. Parshamoni, S. Sanda, H. S. Jena and S. Konar, *Chem Asian J*, 2015, **10**, 653-660.
49. J. C. Tan, C. A. Merrill, J. B. Orton and A. K. Cheetham, *Acta. Mater.*, 2009, **57**, 3481-3496.
50. N. W. Khun, E. M. Mahdi, S. Q. Ying, T. Sui, A. M. Korsunsky and J. C. Tan, *APL Materials*, 2014, **2**, 124101.
51. A. C. Comer, D. S. Kalika, B. W. Rowe, B. D. Freeman and D. R. Paul, *Polymer*, 2009, **50**, 891-897.
52. S. A. Moggach, T. D. Bennett and A. K. Cheetham, *Angew. Chem. Int. Ed. Engl.*, 2009, **48**, 7087-7089.
53. J. T. Hughes, D. F. Sava, T. M. Nenoff and A. Navrotsky, *J. Am. Chem. Soc.*, 2013, **135**, 16256-16259.
54. Q. Song, S. K. Nataraj, M. V. Roussenova, J. C. Tan, D. J. Hughes, W. Li, P. Bourgoin, M. A. Alam, A. K. Cheetham, S. A. Al-Muhtaseb and E. Sivaniah, *Energy Environ. Sci.*, 2012, **5**, 8359-8369.
55. T. D. Bennett, P. J. Saines, D. A. Keen, J. C. Tan and A. K. Cheetham, *Chem. Eur. J.*, 2013, **19**, 7049-7055.
56. J. T. Hughes, D. F. Sava, T. M. Nenoff and A. Navrotsky, *J. Am. Chem. Soc.*, 2013, **135**, 16256-16259.
57. D. Cangialosi, H. Schut, A. van Veen and S. J. Picken, *Macromolecules*, 2003, **36**, 142-147.
58. S.-H. Huo and X.-P. Yan, *J. Mater. Chem.*, 2012, **22**, 7449.
59. J. O. Hsieh, K. J. Balkus, J. P. Ferraris and I. H. Musselman, *Microporous Mesoporous Mat.*, 2014, **196**, 165-174.
60. A. K. Chaudhari, I. Han and J. C. Tan, *Adv. Mater.*, 2015, **27**, 4438-4446.
61. J. Kahr, R. E. Morris and P. A. Wright, *CrystEngComm*, 2013, **15**, 9779.
62. P. D. Dietzel, P. A. Georgiev, J. Eckert, R. Blom, T. Strassle and T. Unruh, *Chem. Commun.*, 2010, **46**, 4962-4964.
63. H. B. T. Jeazet, C. Staudt and C. Janiak, *Dalton Trans.*, 2012, **41**, 14003-14027.
64. G. X. Dong, H. Y. Li and V. K. Chen, *J. Mater. Chem. A*, 2013, **1**, 4610-4630.

This journal is © The Royal Society of Chemistry 2016

Please do not adjust margins